

True stress and shakedown analysis of pressure vessel under repeated internal pressure

XIAOLIANG-JIA, JING-WANG, YILIANG-ZHANG, GONGFENG-JIANG AND YANJUN ZENG^a

Beijing University of Technology, 100022 Beijing, P.R. China

Received 9 March 2015, Accepted 16 November 2015

Abstract – This study aims to investigate the true stress and the plastic shakedown behavior of a cyclically loaded pressure vessel. To serve this study, an experimental platform has been built up, which comprised of a self-made thin-wall cylinder pressure vessel, a water pressure loading system to simulate the actual working loading condition, and strain gauge sets for strain measurement. A number of experiments have been done by cyclically loading and unloading the vessel at different strain levels of plastic deformation to shakedown state in different experiments respectively. The relationship between plastic strain and shakedown range has therefore been obtained. The true stress-strain constitutive model of the vessel under large deformation condition has also been derived. The experiments lead to three observations: (1) the strain hardening technology can effectively reduce the residual stress of stainless steel pressure vessel. (2) The shakedown range is less than $2000 \mu\epsilon$ for a total strain under 4%, and yet the shakedown range increases fast to more than $3000 \mu\epsilon$ for a total strain higher than 6%. (3) It is also found that the true stress-strain constitutive model given in this paper describes the multi-axial stress-strain state of pressure vessels, and validates the engineering practicability of conventional uniaxial tensile shakedown constitutive curve.

Key words: Strain accumulation / cyclic loading / strain / true stress / strain hardening

1 Introduction

How to establish shakedown design criteria in consideration of strain hardening technology to design pressure vessels has been focused in recent years. Shakedown analysis is a study of plastic behavior of engineering structure subjected to cyclic loading. The shakedown critical load of a structure can be obtained based on shakedown and accumulated plastic strain analysis. A structure cyclically loaded within its critical load will get into shakedown state. If cyclically loading the structure beyond its critical load, an increment plastic collapse or alternating plastic collapse will occur to the structure due to the continuously accumulated plastic strain. Shakedown theory is widely applied to analytical design method of pressure vessels and it has been introduced into ASME VIII-2 [1]. The basic principle of strain hardening technology is that overload the pressure vessel to plastic stage so that the elastic limit of pressure vessels can be improved. However, for a pressure vessel subjected to cyclic loading, the strain accumulation with continuous plastic deformation should be noticed. Hence, it has great theoretical and practical significance to apply shakedown analysis to strain hardening technology.

It is known that an elastic-plastic metallic material subjected to a cyclic loading may reach three different types of steady-state responses after a certain finite number of cycles:

- (1) Elastic shakedown. The plastic accumulation no longer occurs, the plastic strain rate and all internal variable rates vanish and thus the structural response to loads becomes purely elastic due to self-balance residual stress field developed inside the structure.
- (2) Plastic shakedown. The plastic accumulation is a non-trivial one, but the plastic strain field resulting in the cycle is nought, since the plastic strains are periodic in the cycle.
- (3) Ratcheting. The plastic accumulation is a nontrivial one, and the ratchet strain is non-vanishing due to the plastic strain to progressively increase [2–5].

A lot of work on shakedown and ratcheting of different structures and materials [6–18] has been done by Chen et al. etc. Xu has presented a perturbation method for shakedown analysis of elasto-plastic structures under quasi-static loading [19]. Guozheng Kang has developed a unified viscoplastic constitutive model to describe uniaxial ratcheting of 304SS [20]. Press has used a new method to make shakedown analysis of nozzles [21]. Ahmadzadeh has studied the ratcheting response of steel alloys under step-loading conditions [22]. ManSoo Joun

^a Corresponding author: yjzeng@bjut.edu.cn

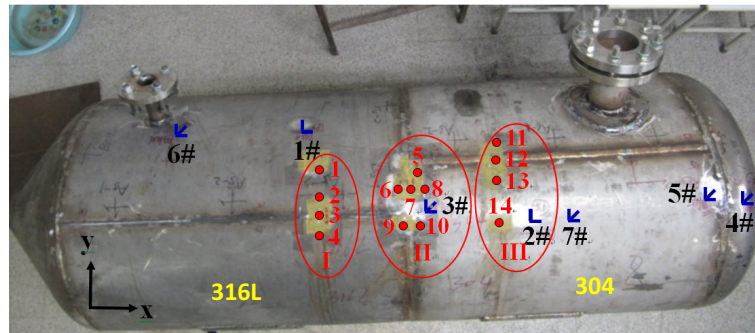


Fig. 1. Experimental pressure vessel.

has presented a new method for acquiring true stress-strain curves over large range of strains using engineering stress-strain curves obtained from a tensile test with a finite element analysis [23]. Masayuki Kamaya has obtained the true stress-strain curves of cold worked stainless steel over a large range of strains by using a specific testing method [24]. Liu has presented that cyclic hardening is one of the factors resulting in shakedown [25]. Although shakedown theory has been discussed in a large number of papers, but few experimental research for pressure vessel shakedown analysis has been published. Meanwhile, how to apply shakedown analysis to strain hardening technology to design pressure vessel is further concerned by more and more scholars.

This paper investigates the relationship between plastic strain and shakedown range, as well as the relationship between plastic strain and residual stress based on experiments. An experimental platform has been built up, which comprised of a water pressure loading system, strain gauge sets for strain measurement, and a thin-wall cylinder pressure vessel to simulate the actual working loading condition. Numerous experiments have been done to get the load and strain of the vessel under cyclic loading and unloading. Therefore, the shakedown strain and the relationship between plastic strain and shakedown range have been obtained. The residual stresses were tested for 6 times during cyclic loading, from which the relationship between plastic strain and residual stresses was obtained. The true stress calculated formulas of pressure vessel under multi-axial stress state were derived. A true stress-strain constitutive model to describe the multi-axial stress-strain state of pressure vessel has been derived from these experiments based on Ramberg-Osgood relationship. Meanwhile, the engineering practicability of conventional uniaxial tensile shakedown constitutive curve has been validated.

2 Experiments

2.1 Experimental design and procedure

2.1.1 Experimental pressure vessel

The left part of the vessel is made of 316L stainless steel and the right part is made of 304 stainless steel.

Chemical composition of 316L is C, 0.026%; Si, 0.72%, P, 0.042%; Ni, 12.5%; Cr, 16.2%; Mo: 2.1%. Chemical composition of 304 is C, 0.046%; Mn 1.21%, P, 0.029%; S, 0.006%; Cr, 17.56%; Ni, 8.07%. The vessel has a length of 1600 mm, diameter of 600 mm and thickness of 5 mm. The experimental vessel, similar with the fabricated in-service vessel, consists of head, tube, manhole, axial welds and circumferential welds (see Fig. 1).

2.1.2 Strain gauge layout scheme and the arrangement of residual stress measuring points

The strain gauges (YEFLA-5) for large strain measurement were used. The special adhesive (NP-50) and advanced UCAM-10A data collector (produced by KYOWA) were applied to guarantee measurement accuracy. Seven strain rosettes were stuck respectively on base material (1#, 2#, 7#), weld heat-affected zone (3#), head (4#, 5#) and tube (6#) of the vessel (see Fig. 1).

The residual stresses were measured by MSF-2 X-ray diffraction stress measurement. As Figure 1 shows, 14 measuring points were arranged respectively on base material, axial welds, circumferential welds and weld heat-affected zone of 316L (part I), the junction of 316L and 304 (part II), and 304 (part III).

2.1.3 Experimental scheme

The strain control method was used to apply the loads and the strain of base material was used as the control criterion. The vessel was loaded to target strain at first and then cyclically loaded and unloaded until it got into shakedown state, which was applied at 9 plastic strain levels of 2.2%, 4.4%, 5%, 5.5%, 6%, 7.3%, 8%, 10%, respectively.

The hoop and axial residual stresses of the vessel were measured for 6 times which was applied at plastic strain levels of 0%, 0.01%, 2.2%, 4.4%, 7.3%, 10%.

2.1.4 Shakedown judgment criterion

In this paper, the ratcheting strain is defined as the maximum strain of each cycle. When the increment of

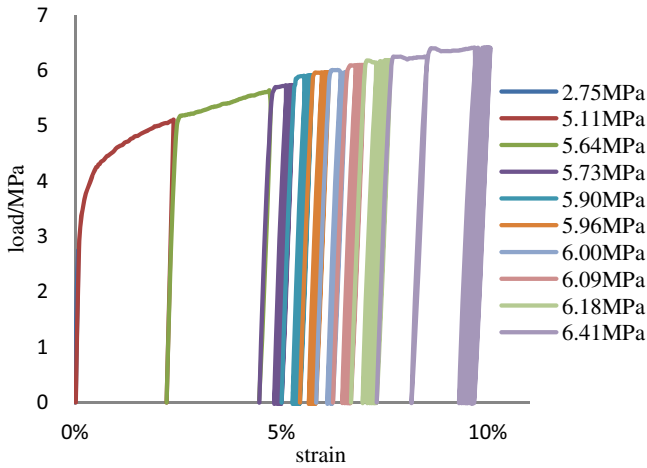


Fig. 2. 316L material (1#) load-strain curve.

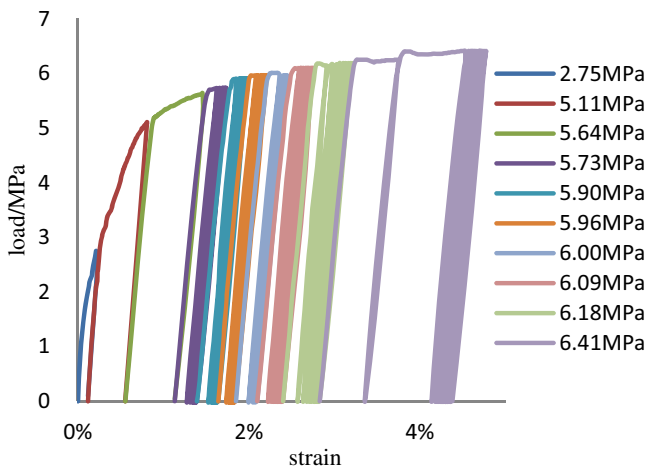


Fig. 3. Weld heat-affected zone (3#) load-stress curve.

ratcheting strain was lower than 20 micro strain, the vessel is considered going in shakedown state. At this time, the ratcheting is considered to stop and the accumulated strain is calculated.

2.2 Experimental results

2.2.1 Strain measurement results

Seven load-strain curves of the vessel subjected to cyclic loading were obtained. Some typical curves are shown in this paper.

The load-strain curve for 316L base material (1#) is shown in Figure 2. The load-strain curve for weld heat-affected zone (3#) is shown in Figure 3.

2.2.2 Residual stress measurement results

According to the residual stresses distribution of the vessel, the hoop residual stress is set as σ_1 , the axial residual stress is set as σ_2 , and $\sigma_3 = 0$.

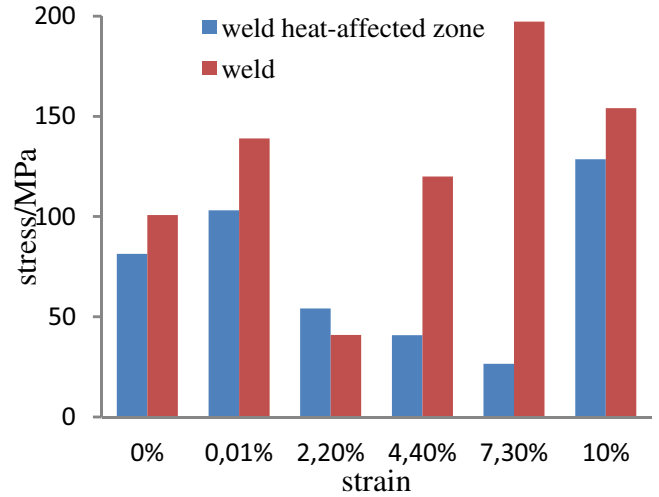


Fig. 4. The residual stresses distribution of I.

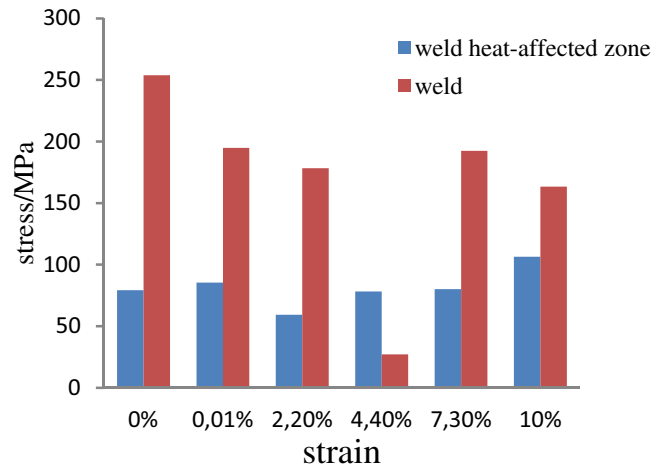


Fig. 5. The residual stresses distribution of II.

Thus, the equivalent Von Mises stress is:

$$\bar{\sigma} = \frac{1}{\sqrt{2}} \sqrt{[(\sigma_1 - \sigma_2)^2 + (\sigma_2 - \sigma_3)^2 + (\sigma_3 - \sigma_1)^2]} \quad (1)$$

The equivalent residual stresses of every heat-affected zone at every plastic level (I: 2# and 4#; II: 6# and 8#, III: 11# and 13#) have been averaged, as shown from Figures 4 to 6. The equivalent residual stresses of weld at every plastic level (I: 3#; II: 7#, III: 12#) are also shown in Figures 4 to 6.

3 Analysis of true stress and strain of the vessel

3.1 Equivalent stress formula of the vessel subjected to cyclic loading

The stress state of a thin-wall cylinder pressure vessel subjected to internal pressure is biaxial stress state. The

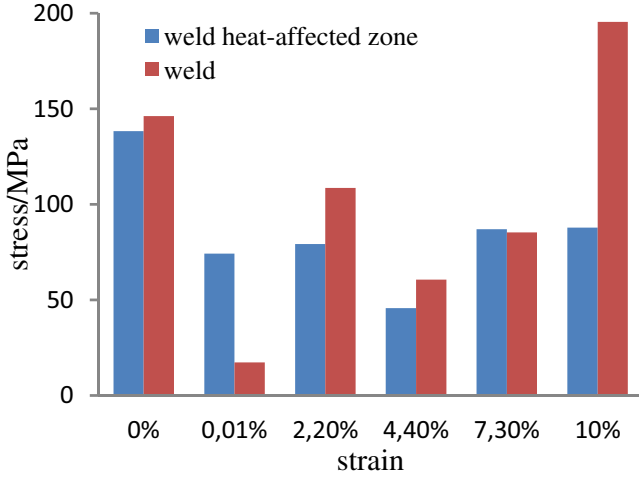


Fig. 6. The residual stresses distribution of III.

stress state is shown as following:

$$\sigma_1 = \sigma_y = \frac{PD}{2t}, \quad \sigma_2 = \sigma_x = \frac{PD}{4t}, \quad \sigma_3 = 0 \quad (2)$$

where σ_x is longitudinal stress; σ_y is hoop stress.

Maximum and minimum principal strain

$$\varepsilon_{1,2} = \frac{\varepsilon_0 + \varepsilon_{90}}{2} \pm \frac{\sqrt{2}}{2} \sqrt{[(\varepsilon_0 - \varepsilon_{45})^2 + (\varepsilon_{45} - \varepsilon_{90})^2]} \quad (3)$$

Equivalent Von Mises strain

$$\bar{\varepsilon} = \frac{\sqrt{2}}{3} \sqrt{[(\varepsilon_1 - \varepsilon_2)^2 + (\varepsilon_2 - \varepsilon_3)^2 + (\varepsilon_3 - \varepsilon_1)^2]} \quad (4)$$

The principal stress (σ_1, σ_2) of measurement points can be obtained by substituting their loading values into Equation (2). Thus, their equivalent stress can be obtained by Equation (1). Hence, the equivalent stress-strain curves for measurement points (1#, 2#, and 7#) subjected to cyclic loading and unloading at different strain levels of plastic deformation to shakedown state can be obtained. Figure 7 shows such a curve for the point (1#).

3.2 True stress experimental formula of the vessel subjected to cyclic loading

When the vessel gets into large deformation condition, the vessel will expand for the accumulated plastic strain, which will result in a bigger diameter and a thinner wall. There will be an error in stress calculation with the use of the theoretical diameter (D) and thickness (T). Therefore, the real diameter and wall thickness of the vessel should be considered for the true stress calculation.

In view of geometric large deformation, the circumferential and axial true stresses are calculated as follows:

$$\tilde{\sigma}_1 = \frac{P\tilde{D}}{2\tilde{t}}, \quad \tilde{\sigma}_2 = \frac{P\tilde{D}}{4\tilde{t}} \quad (5)$$

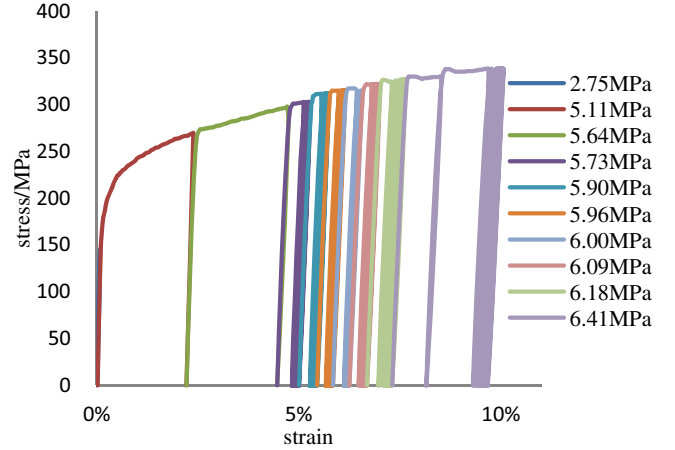


Fig. 7. 316L material (1#) equivalent stress-strain curve.

In this equation, \tilde{D} and \tilde{t} represent the instantaneous diameter and thickness respectively. Plastic mechanics states that pure plastic deformation leads to the change of the vessel's shape, but no change of its volume. Hence, we have

$$I_1 = \varepsilon_1 + \varepsilon_2 + \varepsilon_3 = \varepsilon_x + \varepsilon_y + \varepsilon_z = 0 \quad (6)$$

So:

$$\varepsilon_z = \varepsilon_3 = -(\varepsilon_1 + \varepsilon_2) \quad (7)$$

Variation of thickness:

$$\Delta t = \varepsilon_t t = \varepsilon_z t = -(\varepsilon_1 + \varepsilon_2)t \quad (8)$$

Real thickness:

$$\tilde{t} = t - \Delta t \quad (9)$$

Variation of diameter:

$$\Delta D = \varepsilon_D D = \varepsilon_z D = -(\varepsilon_1 + \varepsilon_2)D \quad (10)$$

Real diameter:

$$\tilde{D} = D + \Delta D \quad (11)$$

The instantaneous real diameter and thickness can be obtained according to equations above. And then the two principal true stresses can be obtained by substituting Equations (8)–(11) into Equation (5):

$$\begin{aligned} \tilde{\sigma}_1 &= \frac{P\tilde{D}}{2\tilde{t}} = \frac{PD(1 + \varepsilon_1 - \varepsilon_2)}{2t(1 + \varepsilon_1 + \varepsilon_2)} \\ \tilde{\sigma}_2 &= \frac{P\tilde{D}}{4\tilde{t}} = \frac{PD(1 - \varepsilon_1 - \varepsilon_2)}{4t(1 + \varepsilon_1 + \varepsilon_2)} \end{aligned} \quad (12)$$

where $\varepsilon_1, \varepsilon_2$ represent the two principal strains. Then the equation of equivalent true stress can be obtained by substituting terms in Equation (12) to Equation (1):

$$\bar{\sigma} = \frac{1}{\sqrt{2}} \sqrt{[(\tilde{\sigma}_1 - \tilde{\sigma}_2)^2 + (\tilde{\sigma}_2 - \tilde{\sigma}_3)^2 + (\tilde{\sigma}_3 - \tilde{\sigma}_1)^2]} \quad (13)$$

Therefore, the true stress-strain curve of the vessel subjected to cyclic loading can be obtained based on the above analysis. The true stress-strain curve of measurement point (1#) is shown in Figure 8.

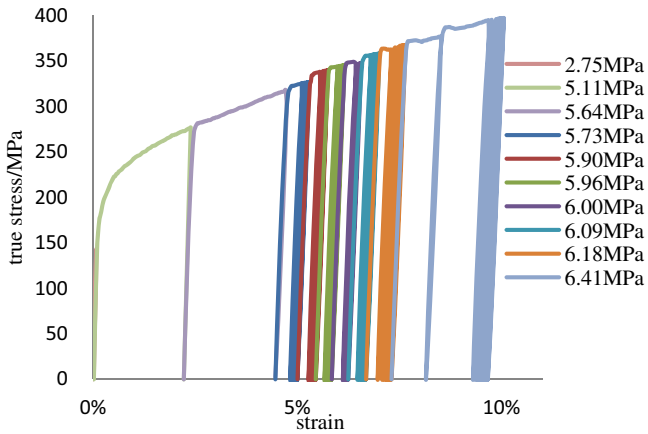


Fig. 8. 316 material 1# true stress-strain curve.

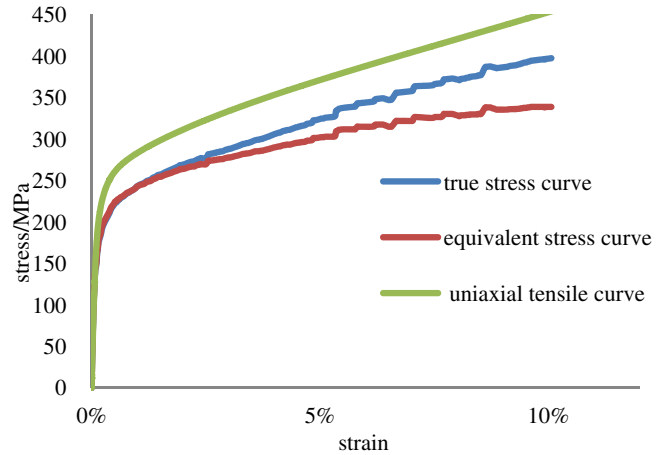


Fig. 9. Equivalent stress-strain and true stress-strain curve.

3.3 The relationship between true stress and equivalent stress under large deformation

The equivalent stress-strain curve and true stress-strain curve of measurement point (1#) subjected to cyclic loading at different strain levels of plastic deformation to shakedown state were put together into one graph for comparative analysis (see Fig. 9). In this paper, the true stress-strain curve of the vessel subjected to cyclic loading to shakedown state is defined as multiaxial cyclic shakedown constitutive curve. The general uniaxial tensile true stress-strain constitutive curve of 316L is also shown in Figure 9 to investigate the difference between multiaxial cyclic shakedown constitutive curve and general uniaxial tensile constitutive curve.

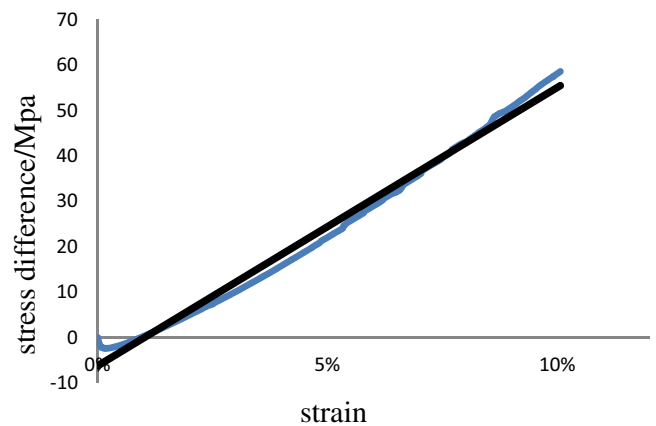


Fig. 10. Stress difference-strain curve.

3.3.1 The difference between true stress-strain curve and equivalent stress-strain curve of 316L

The equivalent stress-strain curve and the true stress-strain curve are almost identical for a total plastic strain less than 2%, and yet the difference between true stress and equivalent stress increases to 17.1% when the total plastic strain reached 10%. Therefore, the influence of large plastic deformation on stress state cannot be ignored in this condition (see Fig. 9).

The difference between true stress and equivalent stress of measurement point (1#) was obtained and was plotted along with the corresponding strain in Figure 10. The curve can be fitted by the following equation:

$$\Delta\sigma = 613.55\varepsilon - 6.25 \quad (14)$$

Equation (4) reveals that the difference between true stress and equivalent stress increases linearly as the accumulated plastic strain increases. Hence, the concept of true stress is important for strength check of pressure vessel under large deformation.

3.3.2 The difference between multiaxial cyclic shakedown constitutive curve and general uniaxial tensile constitutive curve

As Figure 9 shows, the difference between multiaxial cyclic shakedown constitutive curve and general uniaxial tensile constitutive curve is significant in plastic phase. Due to the ratcheting in cyclic loading, the plastic strain accumulates continuously. Therefore, the multiaxial cyclic shakedown constitutive curve is lower than the general uniaxial tensile constitutive curve.

3.4 The true stress-strain constitutive model under large deformation

The true stress-strain constitutive curve of 316 base material is obtained and the mathematical model is deduced in Figure 9. As Figure 9 shows, the offset yield stress ($\sigma_{0.2}$) of the vessel under cyclic loading is 188 MPa; modulus of elasticity is 210 GPa.

The Ramberg-Osgood equation is usually used to describe the stress-strain curve of nonlinear materials, such

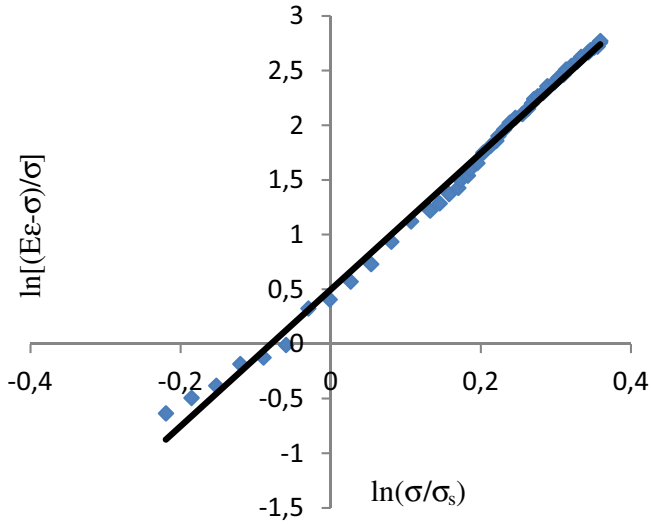


Fig. 11. αn calibration curve.

as stainless steel [26,27]. It is shown as follows:

$$\begin{aligned} \varepsilon &= \varepsilon_e + \varepsilon_p, \quad \varepsilon_e = \frac{\sigma}{E}, \quad \varepsilon_p = \alpha \frac{\sigma}{E} \left(\frac{\sigma}{\sigma_s} \right)^n \\ \varepsilon &= \frac{\sigma}{E} + \alpha \frac{\sigma}{E} \left(\frac{\sigma}{\sigma_s} \right)^n \end{aligned} \quad (15)$$

where ε is the total strain, ε_e is elastic strain, ε_p is plastic strain, σ is stress, σ_s is yield stress, E is modulus of elasticity, α and n are constants that depend on the material being considered.

MacDonald et al. [28–30] presented that Equation (15) can accurately describe the true stress-strain constitutive curve when the total strain is less than 2%, yet the true stress-strain curve indicates the obvious linear relationship when the total strain is more than 2%. It is shown as follows:

$$\varepsilon = \begin{cases} \frac{\sigma}{E} + \alpha \frac{\sigma}{E} \left(\frac{\sigma}{\sigma_s} \right)^n & \sigma \leq \sigma_{2.0} \\ \frac{\sigma - a}{b} & \sigma > \sigma_{2.0} \end{cases} \quad (16)$$

where a and b are constants that depend on the material being considered.

Taking natural logarithm of Equation (15), it can be obtained:

$$\ln \frac{E\varepsilon - \sigma}{\sigma} = \ln \alpha + n \ln \frac{\sigma}{\sigma_s} \quad (17)$$

Substituting the measurement point (1#) experimental data of stress and strain ($0.2\% < \varepsilon < 2.0\%$) into Equation (17). Then, the function curve of Equation (17) is plotted in Figure 11 with $\ln(\sigma/\sigma_s)$ as horizontal coordinate and $\ln[(E\varepsilon-\sigma)/\sigma]$ as vertical coordinate. After that, it is fitted by linear model, as shown in the following:

$$\ln \frac{E\varepsilon - \sigma}{\sigma} = 0.5287 + 6.1117 \ln \frac{\sigma}{\sigma_s} \quad (18)$$

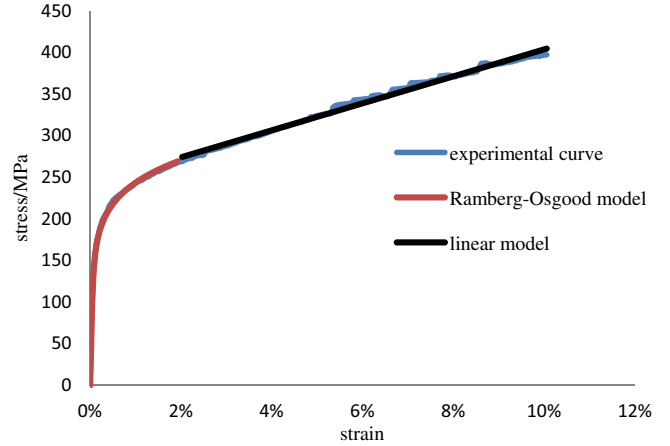


Fig. 12. True stress-strain constitutive curve theoretical model.

It can be obtained from Equation (18): $n = 6.1117$, $\alpha = e^{0.5287} = 1.6967$.

The true stress-strain curve of measurement point (1#) is fitted by linear model with $\varepsilon > 2.0\%$. The result is shown as follows:

$$\sigma = 1623.4\varepsilon + 241.23 \quad (19)$$

Therefore, the theoretical true stress-strain constitutive model of 316L subjected to cyclic loading is obtained as shown in the following:

$$\varepsilon = \begin{cases} \frac{\sigma}{210000} + 1.6967 \times \frac{\sigma}{210000} \left(\frac{\sigma}{188} \right)^{6.1117} & \sigma \leq \sigma_{2.0} \\ \frac{\sigma - 241.23}{1623.4} & \sigma > \sigma_{2.0} \end{cases} \quad (20)$$

The theoretical true stress-strain constitutive curve based on Equation (20) and the experimental true stress-strain constitutive curve of 316L base materials (measurement point 1#) are put together into Figure 12. It can be seen from Figure 12 that the experimental curve is well agreeable with the theoretical curve got by Equation (20).

4 The shakedown analysis of the vessel and the engineering application of ratcheting

4.1 The relationship between the total strain and shakedown range

Figures 2 and 3 show that the occurrence of ratcheting is obvious when the vessel is subjected to cyclic loading and unloading to shakedown state. It can be seen that the ratcheting strain gets lower and lower with cyclic loading and unloading until the vessel gets into shakedown state. In this paper, the shakedown range is defined as the accumulated plastic strain of the vessel when it gets to shakedown state in each experiment (see Fig. 13). The relationship between total strain and shakedown range is

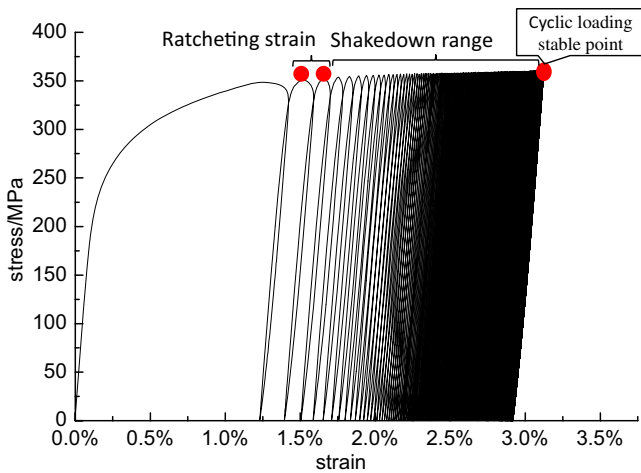


Fig. 13. Cyclic stress-strain stable point definition.

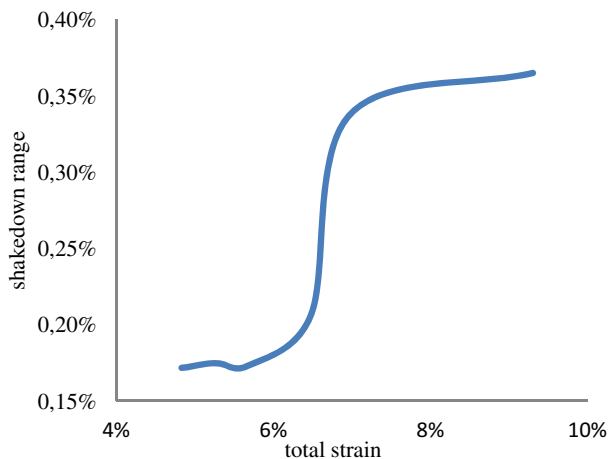


Fig. 14. Shakedown range and total strain.

shown in Figure 14, which shows the shakedown range increases obviously with the total strain. The increase rate of the shakedown range is very low at the beginning, but it increases sharply when the total strain reaches $60\,000\ \mu\epsilon$; and it gets into a steady state again at the $80\,000\ \mu\epsilon$. This phenomenon occurs to both the base material and weld heat-affected zone and can be summarized that both the cycles to reach shakedown state and the shakedown range increase with the increase of strain level when the vessel is subjected to cyclic loading and unloading to shakedown state.

4.2 The effects of strain hardening on residual stresses

It can be seen from Figures 4 to 6 that the initial residual stress of weld and weld heat-affected zone is about 80–250 MPa. The residual stress decreased at first and then increased with strain hardening. By analyzing experimental data, the residual stress obviously decreased when the total strain of base material reached 2.2%. And, the residual stress reduced by 50%–70% when the total

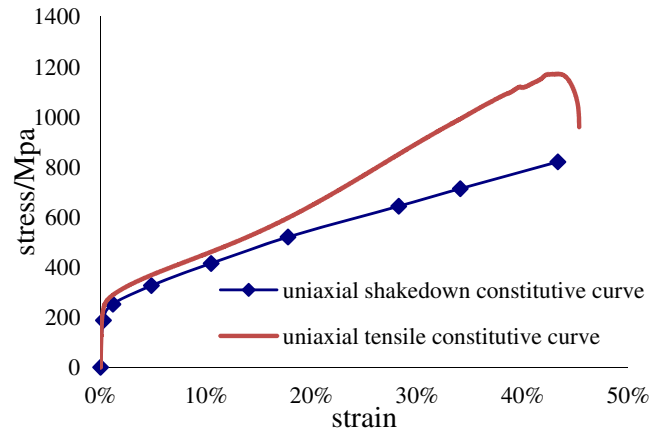


Fig. 15. Uniaxial cyclic constitutive curve.

strain reached 4.4%. Yet, the residual stress obviously increased when the total strain is more than 4.4%. The results show that strain hardening technology can effectively reduce the residual stress of stainless steel pressure vessel. The reduction effect of residual stress is best when the total strain of the vessel reaches 2%–4%.

4.3 The engineering application of ratcheting

In this paper, the cyclic loading stable point is defined as the maximum cyclic stress of the vessel when it gets into shakedown state (see Fig. 13). The shakedown constitutive curve of 316SS subjected to uniaxial cyclic loading and unloading at different strain levels of plastic deformation to shakedown has been obtained by Sun-Liang and JiangGongfeng (see Fig. 15) [31]. This uniaxial cyclic shakedown constitutive curve is composed of stable points at different strain levels of plastic deformation.

The cyclic loading stable points of the vessel subjected to multiaxial cyclic loading were obtained in this study. In order to observe the influence of stress state on constitutive relation, the uniaxial cyclic constitutive curve and the multiaxial cyclic loading stable points were plotted together for comparative analysis (see Fig. 16). In Figure 16 “♦” indicates the uniaxial cyclic shakedown constitutive curve and “×” indicates the multiaxial cyclic shakedown constitutive curve. It can be seen that the uniaxial cyclic constitutive curve and multiaxial cyclic constitutive curve are almost identical when the multiaxial stress is transformed to equivalent stress. Hence, the engineering practicability of conventional uniaxial cyclic loading shakedown constitutive curve is confirmed.

Based on strain hardening technology, in order to improve the proportional limit and reduce residual stresses of pressure vessel as most as possible, the vessel should be loaded under a suitable load to the request plastic strain ($\epsilon_{request}$). As shown in Figures 9 and 15, if the request plastic strain is obtained by single loading, the load of single loading will be greater than the load of cyclic loading. If the ratcheting is considered, the new request plastic

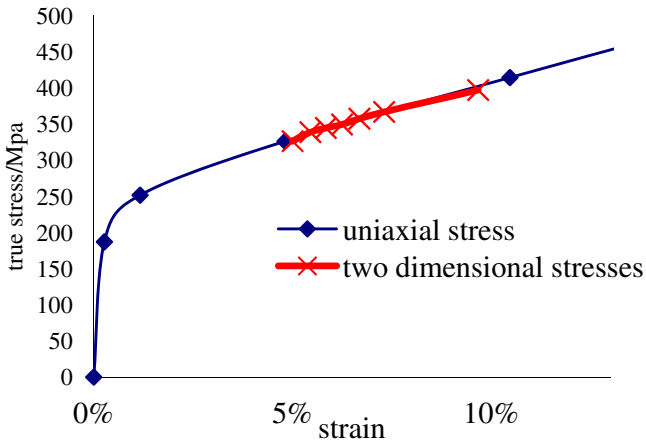


Fig. 16. Uniaxial cyclic curve and multiaxial cyclic curve.

strain ($\epsilon'_{request}$) could be calculated as follows:

$$\epsilon'_{request} = \epsilon_{request} - \epsilon_{ratcheting} \quad (21)$$

In this way, the request plastic strain could be obtained by cyclic loading and unloading according to the shakedown range characteristic. Therefore, the request plastic strain is lowered so that the load is lowered and the risk of overload is reduced.

5 Conclusions

1. Ratcheting effect was observed when the vessel was subjected to cyclic loading and unloading to shakedown state. The shakedown range is proportional to the total strain. The shakedown range is less than $2000 \mu\epsilon$ for a total strain under 4%, and yet the shakedown range increases fast to more than $3000 \mu\epsilon$ for a total strain higher than 6%. The overload risk could be reduced by the application of ratcheting effect.
2. The uniaxial cyclic shakedown constitutive curve and multiaxial cyclic shakedown constitutive curve are well coincident when the multiaxial stress is transformed to equivalent stress, which confirms that the uniaxial cyclic shakedown constitutive curve has practicability in engineering.
3. The strain hardening technology can effectively reduce the residual stress of stainless steel pressure vessel. The residual stress reduced by 50%–70% when the total strain reached 4.4%.
4. The true stress-strain constitutive model of 316 base materials under large deformation is deduced by the following equations:

$$\epsilon = \begin{cases} \frac{\sigma}{210000} + 1.6967 \times \frac{\sigma}{210000} \left(\frac{\sigma}{188}\right)^{6.1117} & \sigma \leq \sigma_{2.0} \\ \frac{\sigma - 241.23}{1623.4} & \sigma > \sigma_{2.0} \end{cases}$$

References

- [1] ASME Boiler and Pressure Vessel Code. American Society of Mechanical Engineers, New York, 2009
- [2] C. Polizzotto, On the conditions to prevent plastic shakedown of structures part 1-Theory, ASME, J. Appl. Mech. 60 (1993) 15–19
- [3] C. Polizzotto, On the conditions to prevent plastic shakedown of structures part 2-The Plastic Shakedown limit load, ASME, J. Appl. Mech. 60 (1993) 20–25
- [4] C. Polizzotto, A Study on Plastic Shakedown of Structures: part 1-Basic Properties, ASME, J. Appl. Mech. 60 (1993) 318–323
- [5] C. Polizzotto, A Study on Plastic Shakedown of Structures: part 2-Theorems, ASME, J. Appl. Mech. 160 (1993) 324–330
- [6] Chen Gang, Numerical theories and engineering methods for structural limit and shakedown analyses, Science Press, Beijing, 2006
- [7] Masatsugu Yaguchi, Yukio Takahashi, Ratchetting of viscoplastic material with cyclic softening, Part 1 experiments on modified 9Cr-1Mo steel, Int. J. Plasticity 21 (2005) 43–65
- [8] I. Scheider, W. Brocks, A. Cornec, Procedure for the Determination of True Stress-Strain Curves From Tensile Test With Rectangular Cross-Section Specimens, J. Eng. Mater. Technol. 126 (2004) 70–76
- [9] M. Kamaya, M. Kawakubo, True stress-strain curves of cold worked stainless steel over a large range of strains, J. Nucl. Mater. 451 (2014) 246–275
- [10] G. Jiang, L. Sun, Y. Liu, G. Chen, A plastic shakedown constitutive curve based on uniaxial ratcheting behavior of 304 stainless steel at room temperature, Fatigue Fracture Eng. Mater. Struct. 37 (2014) 359–367
- [11] M. Abdel-Karim, An extension for the OhnoWang kinematic hardening rules to incorporate isotropic hardening, Int. J. Pres. Ves. Piping 87 (2010) 170–176
- [12] G.Z. Kang, Ratchetting: recent progresses in phenomenon observation, constitutive modeling and application, Int. J. Fatigue 30 (2008) 1448–1472
- [13] Quoc-Son Nguyen, On shakedown analysis in hardening plasticity, J. Mech. Phys. Solids 51 (2003) 101–125
- [14] Pham Duc Chinh, Shakedown static and kinematic theorems for elastic-plastic limited linear kinematic-hardening, Eur. J. Mech. A/Solids 24 (2005) 35–45
- [15] Mohammad, Abdel-Karim, An evaluation for several kinematic hardening rules on prediction of multiaxial stress-controlled ratcheting, Int. J. Plasticity 26 (2010) 711–730
- [16] Haofeng Chen, Weihang Chen, Tianbai Li, James Ure, On Shakedown, Ratchet and Limit Analyses of Defective Pipeline, J. Pressure Vessel Technol. 134 (2011) 1–8
- [17] G.R. Ahmadzadeh, A. Varavani-Farahani, Triphasic ratcheting strain prediction of materials over stress cycles, Fatigue Fracture Eng. Mater. Struct. 35 (2012) 929–935
- [18] G.R. Ahmadzadeh, A. Varavani-Farahani, Ratcheting assessment of steel alloys under step-loading conditions, Mater. Design. 51 (2013) 231–241
- [19] Du Sentian, Xu Bingye, PanLigong, An analysis of the shakedown problem of elasto-plastic structures under Quasi-static loading by the perturbation method, Chinese J. Theoretical Appl. Mech. 23 (1991) 101–125

- [20] Guozheng Kang, Qing Gao, Xianjie Yang, A visco-plastic constitutive model incorporated with cyclic hardening for uniaxial/multiaxial ratcheting of SS304 stainless steel at room temperature, *Mech. Mater.* 34 (2002) 521–531
- [21] R. Preiss, On the shakedown analysis of nozzles using elasto-plastic FEA, *Int. J. Pres. Ves. Piping* 76 (1999) 421–434
- [22] G.R. Ahmadzadeh, A. Varavani-Farahani, Ratcheting assessment of steel alloys under step-loading conditions, *Mater. Design* 51 (2013) 231–241
- [23] ManSoo Joun, Jea Gun Eom, Min Cheol Lee, A new method for acquiring true stress-strain curves over a large of strains using a tensile test and finite element method, *Mech. Mater.* 40 (2008) 586–593
- [24] M. Kamaya, M. Kawakubo, True stress–strain curves of cold worked stainless steel over a large range of strains, *J. Nucl. Mater.* (2014) 246–275
- [25] Liu Feng-lei, Zhang Meng, Wang Bu-kang, Plastic Shakedown Analysis of Metal Material, *Mech. Eng. Automation* 1 (2005) 47–50
- [26] W. Ramberg, W.R. Osgood, Description of stress-strain curves by three parameters, National Advisory Committee for Aeronautics, Washington (DC) Technical note No. 902, 1943
- [27] H.N. Hill, Determination of stress- strain relations from the offset yield strength values, National Advisory Committee for Aeronautics, Washington (DC) Technical note No. 927, 1944
- [28] M. Macdonald, J. Rhodes, G.T. Taylor, Mechanical properties of stainless steel lipped channels, *Proceedings of 15th International Specialty Conference on Cold-Formed Steel Structures*, 2000, pp. 673–686
- [29] A. Olsson, *Stainless Steel Plasticity-Material Modeling and Structural Applications*, Sweden: Lule 1/4 University of Technology, 2001
- [30] W.M. Quach, J.G. Teng, K.F. Chung, Threestage stress-strain model for stainless steel, *J. Struct. Eng. ASCE* 134 (2008) 1518–1527
- [31] G. Jiang , L. Sun, Y. Liu, et al., A plastic shakedown constitutive curve based on uniaxial ratcheting behavior of 304 stainless steel at room temperature, *Fatigue Fracture Eng. Mater. Struct.* 37 (2014) 359–367